Detector Performance for the FIREBall-2 UV Experiment

April D. Jewell,[1*] Erika T. Hamden,[2] Hwei Ru Ong,[3] John Hennessy,[1] Timothy Goodsall,[1] Charles Shapiro,[1] Samuel Cheng,[1] Todd Jones,[1] Alexander Carver,[1] Michael Hoenk,[1] David Schiminovich,[3] Christopher Martin,[2] and Shouleh Nikzad[1]

[1]*Jet Propulsion Laboratory, California Institute of Technology, 4800 Oak Grove Drive, Pasadena, CA 91109, USA*

[2]*Department of Physics, Mathematics and Astronomy, California Institute of Technology, 1200 East California Boulevard, Pasadena, CA 91125, USA*

[3]*Department of Astronomy, Columbia University, 550 West 120th Street, New York, NY 10027, USA*

We present an overview of the detector for the upcoming Faint Intergalactic Red-shifted Emission Balloon (FIREBall-2) experiment, with a particular focus on the development of device-integrated optical coatings and detector quantum efficiency (QE). FIREBall-2 is designed to measure emission from the strong resonance lines of HI, OVI, and CIV, all red-shifted to 195-225 nm window; its detector is a delta-doped electron multiplying charge-coupled device (EM-CCD). Delta-doped arrays, invented at JPL, achieve 100% internal QE from the UV through the visible. External losses due to reflection (~70% in some UV regions) can be mitigated with antireflection coatings (ARCs). Using atomic layer deposition (ALD), thin-film optical filters are incorporated with existing detector technologies. ALD offers nanometer-scale control over film thickness and interface quality, allowing for precision growth of multilayer films. Several AR coatings, including single and multi-layer designs, were tested for FIREBall-2. QE measurements match modeled transmittance behavior remarkably well, showing improved performance in the target wavelength range. Also under development are ALD coatings to enhance QE for a variety of spectral regions throughout the UV (90-320 nm) and visible (320-1000 nm) range both for space-based imaging and spectroscopy as well as for ground-based telescopes.

Keywords: Ultraviolet, EMCCD, AR coating, delta doping, FIREBall, atomic layer deposition

1. FIREBALL-2

The Faint Intergalactic Red Shifted Emission Balloon (FIREBall-2) is a balloon-borne UV spectrograph funded jointly by NASA and CNES. Briefly, FIREBall-2 is designed to observe emission from the circumgalactic medium (CGM), the diffuse gas around galaxies. The primary targets include line emission from HI (Lyman-α, 121.6 nm) at a redshift of z=0.7; OVI (103.3 nm) at z=1.0; and CIV (154.9 nm) at z=0.3. The instrument is optimized for narrowband observations spanning the stratospheric window (200-210 nm) centered at 205 nm. FIREBall-2 is a follow on to FIREBall-1, which was launched on two separate occasions in 2007 and 2009.[1–4] FIREBall-1 was a technical and engineering success, but elucidated the need for lower detection limits and FIREBall-2, resulting in changes to the spectrograph design and the detector. The focus of this manuscript is on the FIREBall-2 detector, specifically development of Electron Multiplying CCDs (EMCCDs) with unprecedented quantum efficiency (QE) within the FIREBall-2 observation band. Details of the spectrograph design and detector noise performance are provided elsewhere, including within these Proceedings.[5,6]

2. FIREBALL-2 DETECTOR

The FIREBall-2 detector development is a collaborative effort shared between the Jet Propulsion Laboratory (JPL), the California Institute of Technology, and Columbia University. The detector is based on e2v's CCD201-20, an electron multiplying charge-coupled device (EMCCD). EMCCDs are conventional CCDs in which one of the register phases is replaced with a high voltage (40-50 V) gain register that multiplies charge prior to readout (Figure

* electronic mail: april.d.jewell@jpl.nasa.gov

UV, X-Ray, and Gamma-Ray Space Instrumentation for Astronomy XIX, edited by Oswald H. Siegmund
Proc. of SPIE Vol. 9601, 96010N · © 2015 SPIE · CCC code: 0277-786X/15/$18 · doi: 10.1117/12.2190167

1).[7] Depending on the applied voltage, EMCCDs can amplify electron signals by several thousand times, effectively eliminating read noise by allowing the device to operate as a photon counter.[8,9] EMCCDs are well suited for the FIREBall-2 experiment, which will map faint targets.

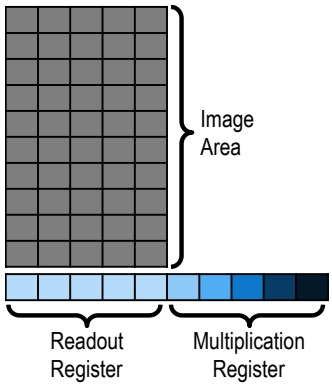

Figure 1. Schematic of an EMCCD showing a conventional CCD architecture with an added multiplication register to amplify signal.

2.1 Two-dimensional doping

Fully fabricated CCD201-20 detector wafers (e2v) were modified for back illumination and to achieve ultraviolet sensitivity. Our post-fabrication process flow has been described elsewhere.[10] Briefly, device wafers are bonded front-side down to a handle wafer (Novati Technologies, Inc.); this handle wafer serves to protect the VLSI fabricated circuitry and pixel structure, and also provides support for the device wafer during and after subsequent thinning steps. The device wafers are then thinned to remove the bulk of the detector substrate by grinding, chemical mechanical polishing, and chemical etching. With these processes, device wafers are thinned from ~800 µm to ~5-10 µm, and have a smooth mirror finish. Additional surface preparation steps are employed to prepare the wafers for epitaxial growth. The thinned device wafer is then passivated by JPL's delta doping process. A highly doped silicon layer is deposited within a nanometer of the substrate surface using low temperature molecular beam epitaxy (MBE).[11,12] In recent years we have extended our work to "superlattice" doping, in which multiple delta layers are deposited within the space of only a few nanometers.[13,14]

JPL's backside thinning and 2D doping processes result in 100% internal quantum efficiency (QE) giving reflection-limited response; detector response can be further improved with antireflection coatings (ARCs).

2.2 Antireflection coatings

ARCs were designed to minimize reflectance (maximize transmittance) across the entire FIREBall-2 band (195-215 nm) with a local minimum at ~205 nm. Several single and multiple layer ARC designs were considered; ARC performance was modeled using TFCalc® (Software Spectra, Inc.) as described elsewhere.[15–17] The finalized ARC design candidates for FIREBall-2 include one, three and five layer coatings, as shown in Table 1. Calculated performance shows that increasing the number of layers within the ARC increases the peak transmittance while also resulting in a narrower peak width, defined here as wavelength range over which transmission ≥50%.

Table 1. Details of the ARC coating designs for the FIREBall-2 detector.

	Coating A	**Coating B**	**Coating C**
Number of Layers	1	3	5
T at 205 nm	64%	74%	81%
Peak Width*	76 nm	40 nm	22 nm

*Defined as wavelength range for which T>50%.

Test coatings were prepared on 1-inch diameter n-type low-resistivity silicon <100> substrates (Virginia Semiconductor, Inc.) using atomic layer deposition (ALD), a thin film growth technique similar to chemical vapor deposition. ALD films are grown a single atomic layer at a time *via* a chemical reaction at the substrate surface. The precursors are introduced to the substrate in two separate steps separated by purges with inert gas (argon, nitrogen, etc.), as shown in Figure 2. This growth technique allows for nanometer scale control of film stoichiometry thickness—typical growth rates are ~1 Å/cycle. For this work, we used a TFS200 ALD system (Beneq) housed in

the Microdevices Laboratory at JPL. Both thermal ALD (tALD) and plasma enhanced ALD (PEALD) were used to prepare Al_2O_3 *via* reactions between trimethylaluminum (TMA, Sigma-Aldrich) and water or oxygen plasma, respectively.[18–22] SiO_2 films were prepared by PEALD using LTO 330 (Air Products) and oxygen plasma.[23,24]

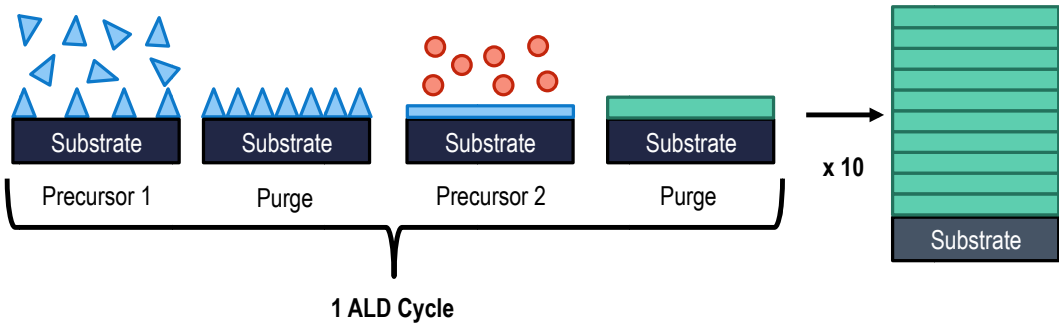

Figure 2. ALD is based on a series of self-limited chemical interactions at the substrate surface. Reactive precursors are deliered in two separate steps separated by purges with inert gas. ALD cycles are repeated to grow the desired film thickness.

The reflectance performance of test coatings prepared on 1-inch silicon substrates was evaluated at Columbia University. The test chamber was fitted with an Acton monochromator with a focused deuterium lamp; reflectance measurements were performed under vacuum ($<1\times10^{-4}$ torr) at near normal angle of incidence (5-10˚). Reflected light intensity was recorded with a photomultiplier tube (Hamamatsu model R6095) with a scintillator and light pipe assembly (McPherson model 658). Several measurements were made for each sample, including direct intensity from the lamp, reflected intensity from the sample and a bare silicon reference, as well as reflected intensity not directly in the path of the light (serves as background). These measurements were used to calculate the direct reflectance of the sample and the silicon reference.

The measured reflectance (R) values for the three test coatings under consideration are shown on the left side in Figures Figure 3-Figure 5 below. The corresponding transmittance (T=100-R) is shown on the right. The measured reflectance matches the model reflectance very well in all three cases. Furthermore, the calculated transmittance matches the model transmittance for λ>210 nm. Both Al_2O_3 and SiO_2 are absorbing lower wavelengths, the model deviates because the TFCalc® software takes film absorbance into account. We previously prepared test coatings on transparent fused silica substrates in order to directly evaluate film absorption.[15] This work showed that reflectance measurements paired with transmittance models provided a good approximation of overall film performance.

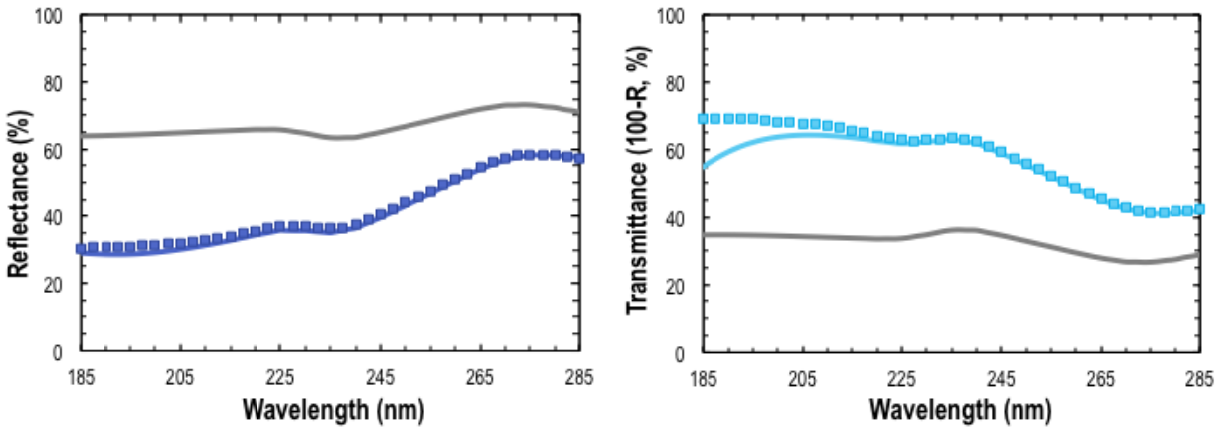

Figure 3. (left) Measured reflectance data (dark blue squares) for Coating A deposited on a silicon test wafer matches model performance (dark blue line). The reflectance of a bare silicon wafer is shown for comparision (grey line). (right) Calculated transmittance (100-R; light blue squares) for Coating A is shown against model transmittance (light blue line). The reflection limited plot for bare silicon is shown for comparison (grey line).

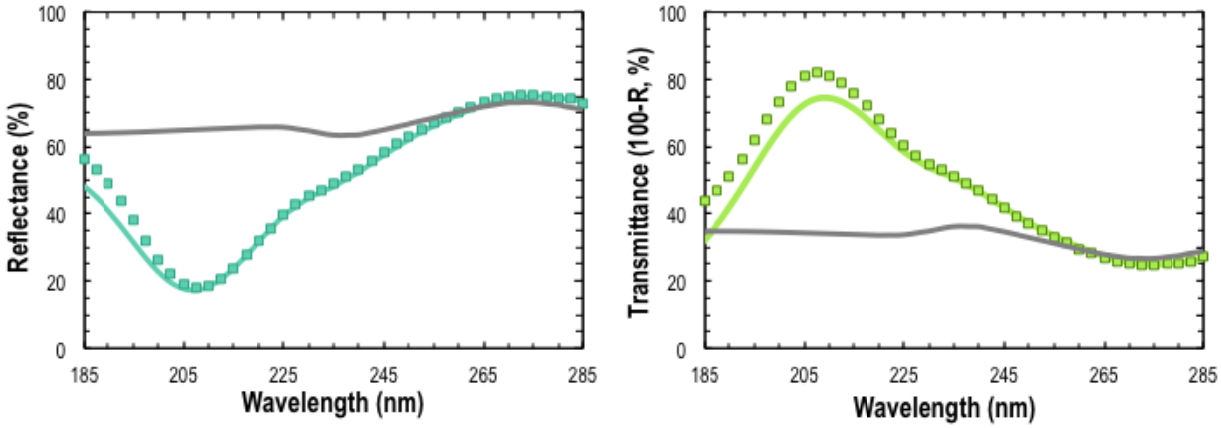

Figure 4. (left) Measured reflectance data (dark green squares) for Coating B deposited on a silicon test wafer matches model performance (dark green line). The reflectance of a bare silicon wafer is shown for comparision (grey line). (right) Calculated transmittance (100-R; light green squares) for Coating B is shown against model transmittance (light green line). The reflection limited plot for bare silicon is shown for comparision (grey line).

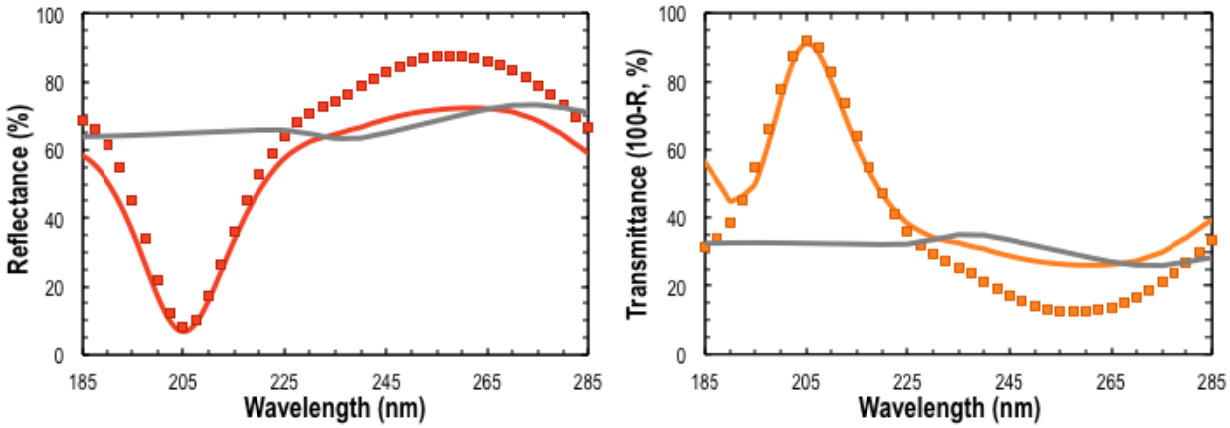

Figure 5. (left) Measured reflectance data (dark orange squares) for Coating C deposited on a silicon test wafer matches model performance (dark orange line). The reflectance of a bare silicon wafer is shown for comparision (grey line). (right) Calculated transmittance (100-R; light orange squares) for Coating C is shown against model transmittance (light orange line). The reflection limited plot for bare silicon is shown for comparision (grey line).

The ARCs described herein are based on single and multiple layer designs, which are based on UV absorbing materials. The films are exceptionally thin (i.e., tens of nanometers) in order to minimize absorption within the individual layers. Furthermore, the FIREBall-2 window is quite narrow, spanning 195-215 nm. Thus, it is exceedingly important that the ARC film thicknesses be accurate to within 5%; otherwise we risk missing our target wavelength. To illustrate this point, several iterations of Coating C were prepared, each with the thickness of the SiO_2 layer interntionally varied. Three samples were prepared as follows: (1) both SiO_2 layers prepared as designed, (2) one SiO_2 layer reduced in thickness by 10% (~3 nm); (3) both SiO_2 layers reduced in thickness by 10%. Reflectance measurements were performed on each of the samples as described above; the results are shown in Figure 6. The peak position clearly shifts towards lower wavelengths and outside of the FIREBall window, even with these modest decreases to ARC film thickness.

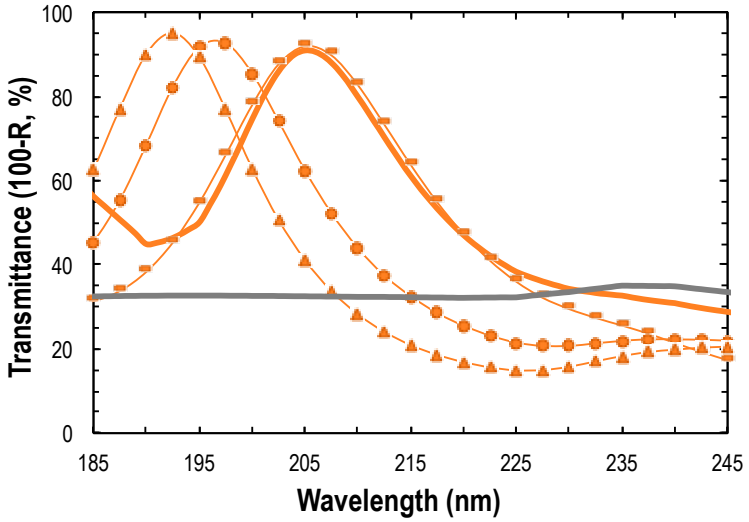

Figure 6. The calcualted transmittance (100-R, measured) of several test coatings is shown against modeled performance (bold solid line) for Coating C. The coatings vary only in the thickness of the two SiO_2 layers within the ARC. The data shows the ARC performance when the layer thicknesses match the design (squares); when one SiO_2 layer is reduced by 3 nm (circles), and when both SiO_2 layers are reduced by 3 nm (triangles). The reflection limited plot for bare silicon is shown for comparision (grey line).

2.3 Detector testing

With test ARC performance verified on bare substrates, each of the ARC designs was deposited on live EMCCD detectors (CCD 201-20, e2v). Packaged detectors with Coatings A, B and C are shown in Figure 7. The color of each detector varies as a result of the ARC performance at visible wavelengths, which will not be discussed here.

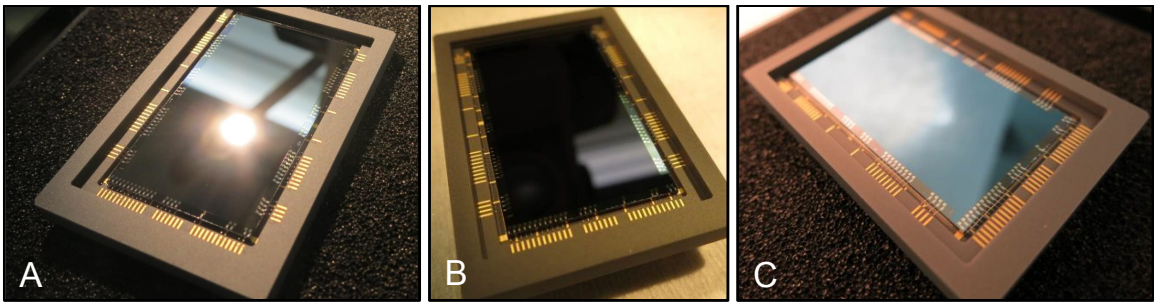

Figure 7. Packaged CCD 201 detectors with Coatings A, B and C applied by ALD. The apparent color of each device is dictated by the ARC behavior at visible wavelengths.

Detector performance of the device with Coating B was evaluated at JPL using a 1-meter Acton monochromator fitted with a both a deuterium lamp and a tungsten halogen lamp, as well as several band pass and long pass filters to reduce wavelength contamination. Details of the characterization set up have previously been described in detail.[25] Detector perfomance matches modeled perfomance quite well in terms of shape and peak position, with the quantum yield (QY) corrected peak QE=57% centered at 210 nm and a peak width of ~20 nm. QY is calculated as photon energy divided by average electron-hole pair energy, where the latter is measured by Kuschnerus et al.[26] The performance of detectors with Coatings A and C will be described in future publications.

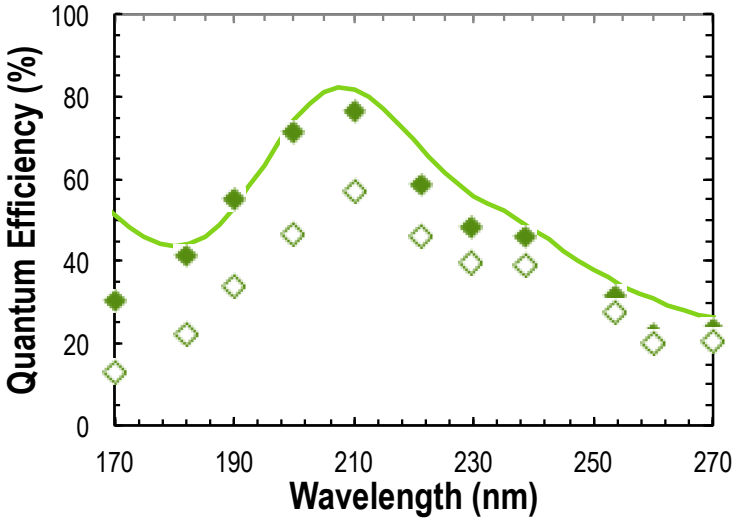

Figure 8. Measured QE (solid diamonds) for a 2D-doped EMCCD with ARC Coating B (three layer design) applied by ALD. The measured data agree well the reflectance data (shown as 100-R) for Coating B (solid line). Also shown is the QY corrected data (open diamonds).

3. FUTURE WORK

The work described herein emphasizes that it is possible to achieve unprecedented QE in the UV with superlattice-doped, AR-coated EMCCDs. The ARC for FIREBall-2 detector was optimized to operate over a relatively narrow wavelength range, restricted by the stratospheric window. However, the 2D doping process can be combined with a variety of ARC designs, enabling detector performance optimization for virtually any wavelength. For future work we will demonstrate EMCCD detectors with >50% QE throughout the UV (100-340 nm). We also will explore ARC patterning techniques so that multiple ARCs can be deposited on a single detector with; thus enabling high performance UV spectroscopy.

4. ACKNOWLEDGMENTS

The research was carried out in part at the Jet Propulsion Laboratory, California Institute of Technology, under a contract with NASA. This work was partially supported the W. M. Keck Institute for Space Studies (KISS) and by NASA Headquarters under NASA Grant NNX11AO07H and NASA Grant NNX12AF29G.

REFERENCES

[1] Tuttle, S. E., Schiminovich, D., Grange, R., Rahman, S., Matuszewski, M., Milliard, B., Deharveng, J.-M., and Martin, D. C., "FIREBALL: the first ultraviolet fiber fed spectrograph," in *Proc. SPIE 7732, Sp. Telesc. Instrum. 2010 Ultrav. to Gamma Ray* **7732**, M. Arnaud, S. S. Murray, and T. Takahashi, Eds., pp. 773227–1 – 15, San Diego (2010).

[2] Milliard, B., Martin, D. C., Schiminovich, D., Evrard, J., Matuszewski, M., Rahman, S., Tuttle, S., McLean, R., Deharveng, J.-M., et al., "FIREBALL: the Faint Intergalactic medium Redshifted Emission Balloon: overview and first science flight results," in *Proc. SPIE 7732, Sp. Telesc. Instrum. 2010 Ultrav. to Gamma Ray* **7732**, M. Arnaud, S. S. Murray, and T. Takahashi, Eds., pp. 773205–1 – 13, San Diego (2010).

[3] Rahman, S., Matuszewski, M., Tuttle, S. E., Vibert, D., Milliard, B., Schiminovich, D., Martin, D. C., Frank, S., Evrard, J., et al., "FIREBALL: detector, data acquisition and reduction," in *Proc. SPIE 7732, Sp. Telesc. Instrum. 2010 Ultrav. to Gamma Ray* **7732**(626), M. Arnaud, S. S. Murray, and T. Takahashi, Eds., pp. 773228–1 – 9, San Diego (2010).

[4] Matuszewski, M., Evrard, J., Mirc, F., Grange, R., Frank, S., Milliard, B., Tuttle, S. E., Rahman, S., Martin, D. C., et al., "FIREBALL: instrument pointing and aspect reconstruction," in *Proc. SPIE 7732, Sp. Telesc. Instrum. 2010 Ultrav. to Gamma Ray* **7732**(626), M. Arnaud, S. S. Murray, and T. Takahashi, Eds., pp. 773229–1 – 9, San Diego (2010).

[5] Hamden, E. T., Lingner, N., Kyne, G., Morrissey, P., and Martin, D. C., "Noise and dark performance for FIREBall-2 EMCCD delta-doped CCD detector," in *Proc. SPIE 9601, UV, X-Ray, Gamma-Ray Sp. Instrum. Astron. XIX*, O. H. Siegmund, S. R. McCandliss, C. Ertley, B. T. Fleming, J. C. Green, and A. Tremsin, Eds., p. 960122, San Diego (2015).

[6] Martin, D. C., Hamden, E. T., Schiminovich, D., Milliard, B., Grange, R., Nikzad, S., Corlies, L., Crabill, R., Ferrand, D., et al., "Fireball-2: a UV multi-object spectrograph for detecting the low z circumgalactic medium," in *Proc. SPIE 9601, UV, X-Ray, Gamma-Ray Sp. Instrum. Astron. XIX*, O. Siegmund, S. R. McCandliss, C. Ertley, B. T. Fleming, J. C. Green, and A. Tremsin, Eds., p. 960120, San Diego (2015).

[7] Jerram, P., Pool, P. J., Bell, R., Burt, D. J., Bowring, S., Spencer, S., Hazelwood, M., Moody, I., Catlett, N., et al., "The LLCCD: low-light imaging without the need for an intensifier," in *Proc. SPIE 4306, Sensors Camera Syst. Sci. Ind. Digit. Photogr. Appl. II*, M. M. Blouke, J. Canosa, and N. Sampat, Eds., pp. 178–186, San Jose (2001).

[8] Daigle, O., Gach, J.-L., Guillaume, C., Carignan, C., Balard, P., and Boisin, O., "L3CCD results in pure photon counting mode," in *Proc. SPIE 5499, Optical and Infrared Detectors for Astronomy*, J. D. Garnett and J. W. Beletic, Eds., pp. 219–227 (2004).

[9] Daigle, O., Djazovski, O., Laurin, D., Doyon, R., and Artigau, É., "Characterization results of EMCCDs for extreme low-light imaging," in *Proc. SPIE 8453, High Energy, Opt. Infrared Detect. Astron. V*, A. D. Holland and J. W. Beletic, Eds., p. 845303, Amsterdam (2012).

[10] Nikzad, S., Hoenk, M. E., Hennessy, J., Jewell, A. D., Carver, A. G., Jones, T. J., Cheng, S. L., Goodsall, T., and Shapiro, C., "High performance silicon imaging arrays for cosmology, planetary sciences, & other applications," in *2014 IEEE Int. Electron Devices Meet.*, pp. 10.7.1–10.7.4, San Francisco (2014).

[11] Hoenk, M. E., Grunthaner, P. J., Grunthaner, F. J., Terhune, R. W., Fattahi, M., and Tseng, H.-F., "Growth of a delta-doped silicon layer by molecular beam epitaxy on a charge-coupled device for reflection-limited ultraviolet quantum efficiency," *Appl. Phys. Lett.* **61**(9), 1084–1086 (1992).

[12] Hoenk, M. E., Grunthaner, P. J., Grunthaner, F. J., Terhune, R. W., and Fattahi, M. M., "Epitaxial Growth of p+ Silicon on a Backside-thinned CCD for Enhanced UV Response," in *Proc. SPIE 1656, High-Resolution Sensors Hybrid Syst.* **1656**(1992), M. M. Blouke, W. Chang, L. J. Thorpe, and R. P. Khosla, Eds., pp. 488–496 (1992).

[13] Hoenk, M. E., Carver, A. G., Jones, T. J., Dickie, M., Cheng, P., Greer, F., Nikzad, S., Sgro, J., and Tsur, S., "The DUV Stability of Superlattice-doped CMOS Detector Arrays," in *Int. Image Sens. Work.*, Snowbird, UT (2013).

[14] Hoenk, M. E., Nikzad, S., Carver, A. G., Jones, T. J., Hennessy, J., Jewell, A. D., Sgro, J., Tsur, S., McClish, M., et al., "Superlattice-doped silicon detectors: progress and prospects," *Proc. SPIE 9154, High Energy, Opt. Infrared Detect. Astron. VI* **9154**, A. D. Holland and J. Beletic, Eds., 915413, Montreal (2014).

[15] Hamden, E. T., Greer, F., Hoenk, M. E., Blacksberg, J., Dickie, M. R., Nikzad, S., Martin, D. C., and Schiminovich, D., "Ultraviolet antireflection coatings for use in silicon detector design," *Appl. Opt.* **50**(21), 4180 (2011).

[16] Hamden, E. T., Jewell, A. D., Shapiro, C. E., Cheng, S. R., Goodsall, T. M., Hennessy, J., Nikzad, S., Hoenk, M. E., Jones, T. J., et al., "CCD Detectors with Greater Than 80% QE at UV Wavelengths," (in preparation).

[17] Hamden, E. T., Jewell, A. D., Gordon, S., Hennessy, J., Hoenk, M. E., Nikzad, S., Schiminovich, D., and Martin, D. C., "High efficiency CCD detectors at UV wavelengths," in *Proc. SPIE 9144, Sp. Telesc. Instrum. 2014 Ultrav. to Gamma Ray*, T. Takahashi, J.-W. A. den Herder, and M. Bautz, Eds., p. 91442X, Montreal (2014).

[18] Heil, S. B. S., van Hemmen, J. L., van de Sanden, M. C. M., and Kessels, W. M. M., "Reaction mechanisms during plasma-assisted atomic layer deposition of metal oxides: A case study for Al2O3," *J. Appl. Phys.* **103**(10), 103302 (2008).

[19] Heil, S. B. S., Kudlacek, P., Langereis, E., Engeln, R., van de Sanden, M. C. M., and Kessels, W. M. M., "In situ reaction mechanism studies of plasma-assisted atomic layer deposition of Al2O3," *Appl. Phys. Lett.* **89**(13), 131505 (2006).

[20] Dingemans, G., Seguin, R., Engelhart, P., Sanden, M. C. M. Van De, and Kessels, W. M. M., "Silicon surface passivation by ultrathin Al2O3 films synthesized by thermal and plasma atomic layer deposition," *Phys. Status Solidi RLL* **4**, 10–12 (2010).

[21] Puurunen, R. L., "Surface chemistry of atomic layer deposition: A case study for the trimethylaluminum/water process," *J. Appl. Phys.* **97**(12), 121301 (2005).

[22] Rai, V. R., Vandalon, V., and Agarwal, S., "Surface reaction mechanisms during ozone and oxygen plasma assisted atomic layer deposition of aluminum oxide.," *Langmuir* **26**(17), 13732–13735 (2010).

[23] Putkonen, M., Karwacki, E. J., and Buchanan, I., "Pushing the Limits in ALD Prosessing Speed," in *Beneq, AirProducts* (2012).

[24] Putkonen, M., Bosund, M., Ylivaara, O. M. E., Puurunen, R. L., Kilpi, L., Ronkainen, H., Sintonen, S., Ali, S., Lipsanen, H., et al., "Thermal and plasma enhanced atomic layer deposition of SiO2 using commercial silicon precursors," *Thin Solid Films* **558**, 93–98, Elsevier B.V. (2014).

[25] Jacquot, B. C., Monacos, S. P., Hoenk, M. E., Greer, F., Jones, T. J., and Nikzad, S., "A system and methodologies for absolute quantum efficiency measurements from the vacuum ultraviolet through the near infrared.," *Rev. Sci. Instrum.* **82**(4), 043102 (2011).

[26] Kuschnerus, P., Rabus, H., Richter, M., Scholze, F., Werner, L., and Ulm, G., "Characterization of photodiodes as transfer detector standards in the 120 nm to 600 nm spectral range," *Metrologia* **35**(4), 355–362 (2003).